Development 119, 485-499 (1993)
Printed in Great Britain © The Company of Biologists Limited 1993



# Defects in heart and lung development in compound heterozygotes for two different targeted mutations at the N-*myc* locus

**Cecilia B. Moens[1,3], Brian R. Stanton[2], Luis F. Parada[2] and Janet Rossant[1,3,*]**

[1]Division of Molecular and Developmental Biology, Samuel Lunenfeld Research Institute, 600 University Ave, Toronto, Ontario, M5G 1X5, Canada
[2]Molecular Embryology Section, ABL-Basic Research Program, National Cancer Institute - Frederick Cancer Research and Development Center, Frederick, Maryland 21702-1201, USA
[3]Department of Molecular and Medical Genetics, University of Toronto

*Author for correspondence

## SUMMARY

**Two types of mutant allele, one leaky and one null, have been generated by gene targeting at the N-*myc* locus in embryonic stem cells and the phenotypes of mice homozygous for these mutations have been described. These mutations have shown that N-*myc* has a number of functions during development, including a role in branching morphogenesis in the lung, which manifests itself at birth in mice homozygous for the leaky allele, and roles in the development of the mesonephric tubules, the neuroepithelium, the sensory ganglia, the gut and the heart, which become evident at midgestation in embryos homozygous for the null allele. In an attempt to define roles for N-*myc* at other stages of development, we have combined the two types of N-*myc* mutant allele in a compound heterozygote that as a result contains approximately 15% of normal levels of N-Myc protein. Compound heterozygotes died during gestation at a time intermediate to the times of death of embryos homozygous for either mutation individually, and their death appeared to result from cardiac failure stemming from hypoplasia of the compact subepicardial layer of the myocardium. Investigation of the expression pattern of N-*myc* and various markers of differentiation in wild-type and compound heterozygote mutant hearts has suggested that N-*myc* may function in maintaining the proliferation and/or preventing the differentiation of compact layer myocytes. This study illustrates the importance of generating different mutations at a given locus to elucidate fully the function of a particular gene during development.**

Key words: N-myc, heart development, targeted mutagenesis, mouse mutant

## INTRODUCTION

N-*myc* is a member of the *myc* family of proto-oncogenes, which includes N-*myc*, c-*myc*, and L-*myc*. Myc proteins are site-specific DNA-binding proteins (Blackwell et al., 1990; Prendergast and Ziff, 1991; Alex et al., 1992), belonging to the basic-helix-loop-helix class of transcription factors, which includes genes that control cell fate determination in such diverse processes as myogenesis, neurogenesis and sex determination (reviewed in Garrell and Campuzano, 1991).

Deregulated expression of *myc* genes has been implicated in the genesis or progression of a number of naturally occurring tumours, in the transformation of cells in culture and in the formation of tumours in transgenic mice (reviewed in DePinho et al., 1991). In general, the sites of expression of a given *myc* gene in vivo reflect the types of tumours associated with its elevated expression. Thus N-*myc* is expressed predominantly in the embryo where it is restricted to undifferentiated subsets of cells in the central and peripheral nervous system, lung, kidney and eye (Mugrauer et al., 1988; Hirning et al., 1991; Zimmerman et al., 1986) and overexpression of N-*myc* has been associated with tumours of embryonic origin such as neuroblastoma (Kohl et al., 1983; Schwab et al., 1983), small-cell lung cancer (Nau et al., 1986; Wong et al., 1986), Wilm's tumour (Nisen et al., 1986) and retinoblastoma (Lee et al., 1984). N-*myc* is also expressed in the skin (Mugrauer et al., 1988), in the epithelial layer of the intestine (Hirning et al., 1991) and, earlier in development, in the heart, sclerotome and visceral arches (Katoh et al., 1991).

The functioning of a Myc protein in vivo should depend not only on its own level of expression, but also on the levels of Max, a protein which, like the Myc proteins, possesses a basic-helix loop helix-leucine zipper (bHLH-LZ) domain (Blackwood and Eisenman, 1991), and which associates with N-Myc, L-Myc and c-Myc proteins in vivo (Blackwood et al., 1992; Wenzel et al., 1991; Mukherjee et al., 1992). Max is required for specific DNA binding by Myc proteins (Blackwood and Eisenman, 1991; Prendergast and Ziff, 1991; Kato et al., 1992; Barrett et al., 1992), and has

been shown to be required for transcriptional activation (Amati et al., 1992) and transformation (Amati et al., 1993) by c-*myc*. Unlike Myc proteins, Max is able to form homodimers in vitro and thereby to bind the *myc*-binding site (Prendergast and Ziff, 1991; Kato et al., 1992). However Max does not transactivate downstream genes on its own (Amati et al., 1992; Kretzner et al., 1992) because it lacks a transactivation domain (Kato et al., 1992) which Myc proteins possess (Kato et al., 1990). Both transformation of fibroblasts by c-*myc* and N-*myc* (Mukherjee et al., 1992; Makela et al., 1992; Prendergast et al., 1992) and transcriptional transactivation by c-*myc* (Amati et al., 1992; Kretzner et al., 1992) have been shown to be enhanced by low levels of Max and inhibited by excess Max, suggesting that Myc function is indeed influenced by levels of Max. Recently, bHLH-LZ proteins have been isolated which also bind the Myc recognition site and which suppress transcription as heterodimers with Max (Ayer et al., 1993; Zervos et al., 1993). One of these, Mad (Ayer et al., 1993), has been shown to compete with Myc for Max in vitro and in transfected cells. Thus high levels of expression of Max dimerization partners may indirectly affect Myc function in vivo by competing for available Max protein and for DNA-recognition sites. Finally, Myc function in vivo may be affected by the levels of other Myc proteins (Mukherjee et al., 1992; Resar et al., 1993).

In an effort to understand the function of *myc* genes in embryogenesis, leaky and null mutations were made in N-*myc* in embryonic stem cells by homologous recombination (Charron et al., 1990; Stanton et al., 1990; Sawai et al., 1991; Moens et al., 1992). These mutations have allowed a description of the function of N-*myc* at different stages of development. Mice homozygous for the null mutations die at midgestation (Stanton et al., 1992; Charron et al., 1992) while mice homozygous for the leaky mutation survive until birth, when they die due to a defect in lung branching morphogenesis (Moens et al., 1992). The latter phenotype is consistent with the normal expression of N-*myc* in the developing lung epithelium, and has led us to postulate that N-*myc* plays a role in the response of the lung epithelium to the signals from the lung mesenchyme that induce epithelial branching.

There have been two detailed reports of the phenotype of mice carrying null mutations in N-*myc* (Stanton et al., 1992; Charron et al., 1992). In the homozygous condition, these mutations cause embryonic death at around 11.5 days p.c. and cause hypoplasia in a number of components of the embryo, different aspects of which have been emphasized by the two groups. The developing genitourinary system shows a reduced number of mesonephric tubules in mutant embryos, which is consistent with N-*myc*'s normal expression in the newly induced epithelium of the meso- and metanephric tubules (Katoh et al., 1991; Mugrauer et al., 1988). The genital ridge is also hypoplastic. Stanton et al. (1992) also describe a defect in the development of the stomach and intestine, consistent with N-*myc*'s expression in the epithelium of these tissues (Hirning et al., 1991). Homozygotes also have reduced cranial and spinal ganglia and a thin neuroepithelium in the telencephalon; both of these are sites of N-*myc* expression in the embryo. Finally, homozygotes have a defect in heart development in which the heart appears to cease development at 9.5 days p.c. (Charron et al., 1992) and as a result is poorly compartmentalized and appears not to have undergone the normal epithelial-to-mesenchymal transitions that result in the formation of the septa and valves. This is again consistent with a previous description of N-*myc* expression in the myocardium of the 9.5 day embryo (Katoh et al., 1991).

By combining leaky and null alleles of N-*myc* in a compound heterozygote, we hoped to investigate N-*myc* function in the mouse embryo at a stage intermediate to those identified by the null and leaky alleles individually. We find that compound heterozygotes indeed survive longer than null homozygotes, but that they die before birth. The mutant phenotype includes a more severe defect in branching morphogenesis of the lung, as well as a cardiac myocyte hypoplasia in the compact subepicardial layer of the ventricular myocardium. We show that, consistent with this phenotype, N-*myc* expression in the developing myocardium is restricted to the compact layer. A role for *myc* genes in the control of myocyte differentiation in the heart is discussed.

## MATERIALS AND METHODS

### PCR genotyping of embryos

Yolk sacs from dissected embryos were washed several times in fresh PBS and placed in 100-200 μl of proteinase K buffer with non-ionic detergents (50 mM KCl, 10 mM Tris pH 8.3, 2.0 mM $MgCl_2$, 0.1 mg/ml gelatin, 0.45% Nonidet P-40, 0.45% Tween-20). 10 μg of proK was added to each tube and samples were incubated at 55°C overnight. 10 μl of the mixture was placed in a PCR tube with 30 μl sterile water and heated to 94°C for 10 minutes before cooling to 62°C. 0.1 μg of each primer, 200 μM dNTPs, 10× reaction buffer and Taq polymerase (Promega) were added and PCR was run with an annealing temperature of 62°C (1 minute), an extension temperature of 72°C (2 minutes), and a denaturing temperature of 94°C (1 minute). Each consecutive cycle was extended by 2 seconds. The oligonucleotide primers used for the PCR detection of 9a, BRP and wild-type alleles of N-*myc* are shown in Fig. 1. Their sequences are as follows: primer a (N-*myc* intron 1): 5′-GGTAGTCGCGCTAGT AAGAG-3′; primer b (N-*myc* exon 2): 5′-GGCGTGGGCA GCAGCTCAAAC-3′; primer c (N-*myc* intron 2): 5′-CCGAGCATCTGTCGCCAAGTC-3′; primer d (neo): 5′-GACCGCTATCAGGACATAGCG-3′.

### Western blotting

An anti-human N-*myc* monoclonal antibody, NCMII 100 (Ikegaki et al., 1986), was generously provided by Dr R. Kennett. 11.5 days p.c. embryos from 9a/+×BRP/+ crosses were dissected and homogenized in several volumes of 1× sample buffer without bromophenol blue (60 mM Tris, pH 6.8, 2% SDS, 0.1 M DTT, 0.32% pharmalyte 3-10 (Pharmacia)). Samples were boiled for 5 minutes and chromosomal DNA was sheared by repeated passage through a 26-gauge needle before freezing at −20°C for future use. Yolk sacs were washed several times in PBS and were prepared for and typed by PCR as described above. After typing, extracts of embryos of each genotype were pooled and the concentration of protein in each sample was determined by the Bradford assay (protein assay reagent from Biorad). Approximately 20 μg of protein from each genotype in 2× loading buffer (0.1 M Tris pH 6.8, 20% glycerol, 4% SDS, 0.2% bromophenol blue, 0.2 M DTT) was run in a 10% SDS-PAGE. Protein was transferred onto PVDF membrane (Immobilon-P, Millipore). Application of primary antibody and fixation of the primary antibody to the blot with 0.2%

glutaraldehyde was performed as described (Ikegaki and Kennett, 1989). Horseradish peroxidase-conjugated goat anti-mouse secondary antibody and reagents for the chemiluminescent detection of HRP activity were obtained in the ECL western blotting kit (Amersham) and were used as suggested by the manufacturer.

### Histology

Dissected embryos were fixed in 10% buffered formalin overnight at room temperature, then were dehydrated and cleared by soaking sequentially in 70%, 80%, 90% and 95% ethanol, 1:1 ethanol:xylene, xylene, 1:1 xylene:paraffin wax, (TissuePrep 2, Fisher Scientific) each for 1 hour. Embryos were then oriented and embedded in paraffin wax. Mutant embryos and control littermates were oriented either for sagittal or frontal sections. 5 μm sections were placed on slides, which were dried overnight at 37°C. Slides were dewaxed, rehydrated, and stained with hematoxylin and eosin. To analyse mutant phenoypes, sections throughout wild-type and mutant embryos were carefully examined in order to find those sections that passed through corresponding regions of the different embryos. Mutant embryos were always compared to non-mutant littermates rather than to non-mutant embryos from other litters, in order to rule out differences due to age.

### RNA in situ hybridizations

Probes for in situs were as follows. N-*myc*: a 541 bp *Pst*1-*Sca*1 fragment of the N-*myc* genomic clone N7.7 (DePinho et al., 1986), including largely 3′-untranslated sequence; c-*myc*: a 351 bp *Hae*III fragment including the untranslated first exon (Bossone et al., 1992); *flk-1:* an 800 bp fragment spanning the transmembrane domain and part of the extracellular ligand-binding domain (Yamaguchi et al., 1993) and α-cardiac actin, a 130 bp *Bam*HI fragment including the first untranslated exon of the mouse α-cardiac actin gene (Sassoon et al., 1988). In situ hybridization was carried out essentially as described (Frohman et al., 1990) with the following modifications: in vitro-transcribed, α-$^{35}$S-labeled RNA probes were used at $5\times10^4$ disintegrations/minute per 1 μl of hybridization solution for the α-cardiac actin probe, and at $1\times10^5$ disintegrations/minute per 1 μl of hybridization solution for c-*myc*, N-*myc* and *flk-1* probes. Slides were hybridized at 53°C overnight, and were washed in the presence of 0.1% β-mercaptoethanol as a reducing agent. High stringency washes were in 50% formamide, 0.1% β-mercaptoethanol, and 1× SSC at 65°C. Final rinses in 2× and 0.1× SSC were at 65°C for 15 minutes. Slides were exposed for either 6 days (for α-cardiac actin probe) or for 14 days (for N-*myc*, *flk-1* and c-*myc* probes). After developing and photographing with dark-field illumination, slides were stained with hematoxylin and eosin and were rephotographed with bright-field illumination.

## RESULTS

### Time of death of N-*myc* compound heterozygotes

The leaky mutation that was generated in N-*myc* (Moens et al., 1992) was termed N-$myc^{9a}$ and the null allele of N-*myc* used in this study was named N-$myc^{BRP}$ (Stanton et al., 1992). Both the N-$myc^{9a}$ mutation and the N-$myc^{BRP}$ mutation are lethal in the homozygous condition. Therefore, N-$myc^{9a/BRP}$ embryos were generated by crossing N-$myc^{9a/+}$ females to N-$myc^{BRP/+}$ males, with the expected ratio of embryos being 1 N-$myc^{+/+}$: 1 N-$myc^{9a/+}$: 1 N-$myc^{BRP/+}$: 1 N-$myc^{9a/BRP}$. The reciprocal cross was also performed: no differences in mutant phenotypes were observed.

In order to expedite the genotypic analysis of offspring from this cross, a PCR strategy was designed that used four oligonucleotide primers to distinguish 9a, BRP, and wild-type alleles of N-*myc* (Fig. 1). 161 live offspring from N-$myc^{9a/+}$×N-$myc^{BRP/+}$ crosses were typed by PCR between 1 day and 3 weeks after birth. Among these pups, 59 were N-$myc^{+/+}$, 53 were N-$myc^{9a/+}$ and 49 were N-$myc^{BRP/+}$. No live animals were N-$myc^{9a/BRP}$. No pups were observed to die postnatally as occurred in the case of N-$myc^{9a/9a}$ newborns, suggesting that the N-$myc^{9a/BRP}$ phenotype was indeed more severe than the N-$myc^{9a/9a}$ phenotype.

We dissected embryos from N-$myc^{9a/+}$×N-$myc^{BRP/+}$ crosses at various stages of gestation in order to determine the time during gestation when N-$myc^{9a/BRP}$ embryos died. Between 8.5 and 11.5 days p.c., N-$myc^{9a/BRP}$ embryos were phenotypically normal and constituted approximately 25% of the total number of embryos, by PCR analysis. Of 268 embryos dissected between 8.5 and 11.5 days p.c., 61 (23%) were N-$myc^{9a/BRP}$ embryos. This is clearly different from the situation in N-$myc^{BRP/BRP}$ embryos, which were all found to be dead by 11.5 days p.c. (Stanton et al., 1992). The observed differences in phenotype among the various mutants were unlikely to be due to different genetic background effects, since all mutant phenotypes were analysed in outbred mice.

Occasionally, N-$myc^{9a/BRP}$ embryos at 11.5 days were slightly smaller than their littermates but were otherwise indistinguishable from their wild-type or single heterozygote littermates. However, by 12.5 days, most N-$myc^{9a/BRP}$ embryos were distinguishable from their littermates either because they were dead and necrotic, or because they were alive but had a characteristic edema of the body wall in the neck area (Fig. 2). Subsequent histological analysis identified this swelling as likely being the result of extravasion of fluid from the vascular compartment into the connective tissue, since the jugular veins are dilated in these embryos (Fig. 7g,h). Of 230 embryos dissected at 12.5 days p.c., 42 (18%) were N-$myc^{9a/BRP}$, but among these, 12 were dead and necrotic, 23 had the characteristic edema described above, two were smaller than normal and five were phenotypically normal. After 12.5 days p.c., live N-$myc^{9a/BRP}$ embryos were progressively less frequent and all were phenotypically abnormal. N-$myc^{9a/BRP}$ embryos that survived until 14.5 days p.c. were always smaller than normal and had a large edema in the neck area. Live N-$myc^{9a/BRP}$ embryos were not observed after 14.5 days p.c. Coincident with the loss of N-$myc^{9a/BRP}$ embryos there was an increase in the number of resorptions visible in the uterus. These resorptions were not typed, but presumably were derived from N-$myc^{9a/BRP}$ embryos, since the sum of the number of N-$myc^{9a/BRP}$ embryos and the number of resorptions added up to approximately 25% of the total number of embryos and resorptions at each stage of gestation. These data are shown graphically in Fig. 3.

### N-Myc protein levels in mutant embryos

Although we have previously shown reduced N-*myc* mRNA levels in N-$myc^{9a/9a}$ embryos (Moens et al., 1992), N-Myc protein levels have not been determined in mice bearing either the leaky or the null N-*myc* alleles. In the present study, we have used western blot analysis to assess N-Myc protein levels in embryos with the various N-*myc* genotypes. Fig. 4 shows a western blot performed on

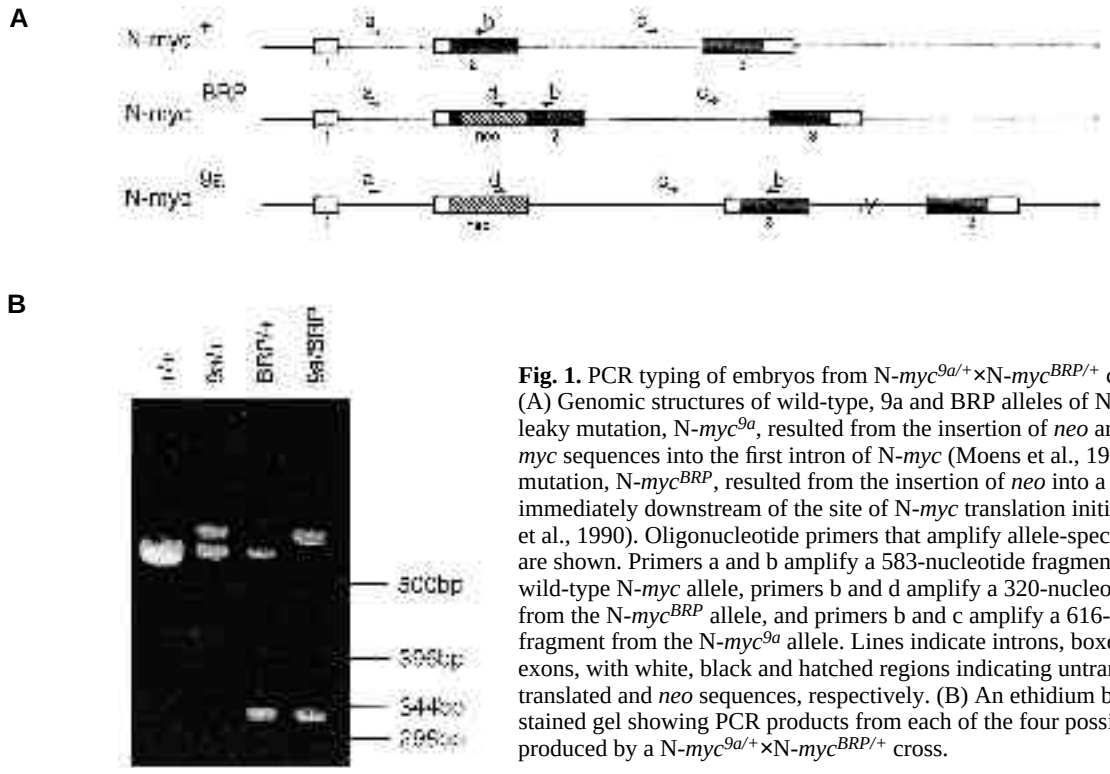


**Fig. 1.** PCR typing of embryos from N-*myc*$^{9a/+}$×N-*myc*$^{BRP/+}$ crosses. (A) Genomic structures of wild-type, 9a and BRP alleles of N-*myc*. The leaky mutation, N-*myc*$^{9a}$, resulted from the insertion of *neo* and flanking N-*myc* sequences into the first intron of N-*myc* (Moens et al., 1992). The null mutation, N-*myc*$^{BRP}$, resulted from the insertion of *neo* into a Xho site immediately downstream of the site of N-*myc* translation initiation (Stanton et al., 1990). Oligonucleotide primers that amplify allele-specific fragments are shown. Primers a and b amplify a 583-nucleotide fragment from the wild-type N-*myc* allele, primers b and d amplify a 320-nucleotide fragment from the N-*myc*$^{BRP}$ allele, and primers b and c amplify a 616-nucleotide fragment from the N-*myc*$^{9a}$ allele. Lines indicate introns, boxes indicate exons, with white, black and hatched regions indicating untranslated, translated and *neo* sequences, respectively. (B) An ethidium bromide-stained gel showing PCR products from each of the four possible genotypes produced by a N-*myc*$^{9a/+}$×N-*myc*$^{BRP/+}$ cross.

extracts of whole 11.5 days p.c. embryos from a N-*myc*$^{9a/+}$×N-*myc*$^{BRP/+}$ cross, using a monoclonal antibody that was raised against human N-Myc protein (Ikegaki et al., 1986), but which also recognizes mouse N-Myc protein. N-Myc protein runs at approximately 65×10$^3$ $M_r$. This N-*myc* antibody also showed binding to a protein of approximately 100×10$^3$ $M_r$. The relative intensities of this cross-reacting band between lanes matched the relative intensities of a ubiquitously expressed protein phosphatase, *syp* (not shown), so this band was used as a loading control in scanning densitometry. The amount of N-Myc protein in N-*myc*$^{9a/BRP}$ embryos was considerably lower than in their wild-type or singly heterozygous littermates. While N-*myc*$^{9a/9a}$ embryos had approximately 25% of wild-type levels of N-Myc protein (not shown), N-*myc*$^{9a/BRP}$ embryos had approximately 15% of wild-type levels, as determined by scanning densitometry of this and several other, similar Western blots. This is consistent with the more severe phenotype of N-*myc*$^{9a/BRP}$ embryos. N-*myc*$^{BRP+}$ embryos had approximately 50% of wild-type levels of N-Myc protein, consistent with the N-*myc*$^{BRP}$ mutation being a null mutation.

## Histological analysis of N-*myc*$^{9a/BRP}$ embryos

In order to determine more precisely the phenotype of N-*myc*$^{9a/BRP}$ embryos, histological analysis of hematoxylin and eosin-stained, sectioned embryos was performed at various stages of development. We examined a total of 42 N-*myc*$^{9a/BRP}$ embryos and 50 N-*myc*$^{+/+}$ littermates in this manner (5 N-*myc*$^{9a/BRP}$ embryos at 14.5 days p.c., 28 at 12.5 days p.c., 3 at 11.5 days p.c., and 6 at 10.5 days p.c.). Younger embryos were analyzed without sectioning, after whole-mount RNA in situ hybridization with various probes (data not shown). Occasionally, N-*myc*$^{9a/+}$ embryos were used as controls since we have previously shown that the N-*myc*$^{9a}$ mutation has no phenotypic effect in the heterozygous condition. N-*myc*$^{9a/BRP}$ embryos not used for histology were used for N-*Myc* protein analysis and RNA in situ analysis.

Before 12.5 days p.c., N-*myc*$^{9a/BRP}$ embryos were apparently normal and could not generally be distinguished from their littermates either by gross morphology or by histological examination of sectioned embryos. The first signs of lethality occurred at 12.5 days, when 12 out of 42 N-*myc*$^{9a/BRP}$ were clearly in the process of resorption. Aside from the edema in the neck area, described above, and their slightly smaller size, live N-*myc*$^{9a/BRP}$ embryos at 12.5 days were still not grossly abnormal. However careful examination of specific organ systems did reveal particular defects.

### Lung development

N-*myc*$^{9a/9a}$ mice die at birth due to a defect in lung branching morphogenesis, consistent with the observation that N-*myc* is expressed in the lung epithelium at early stages of lung development (Moens et al., 1992). Specifically, at 12.5 days p.c., when wild-type lungs have tertiary and quaternary branches, N-*myc*$^{9a/9a}$ lungs had only the beginnings of tertiarybranches. The further reduction in the amount of N-Myc protein in N-*myc*$^{9a/BRP}$ embryos led to an enhancement of this phenotype, as predicted. Branching morphogenesis in N-*myc*$^{9a/BRP}$ lungs was all but blocked (Fig. 5A,B), N-*myc*$^{9a/BRP}$ embryos having only the beginnings of secondary branches. Interestingly, the *pattern* of branching was normal, as can be observed by the presence of a rudimentary right postcaval lobe extending to the left

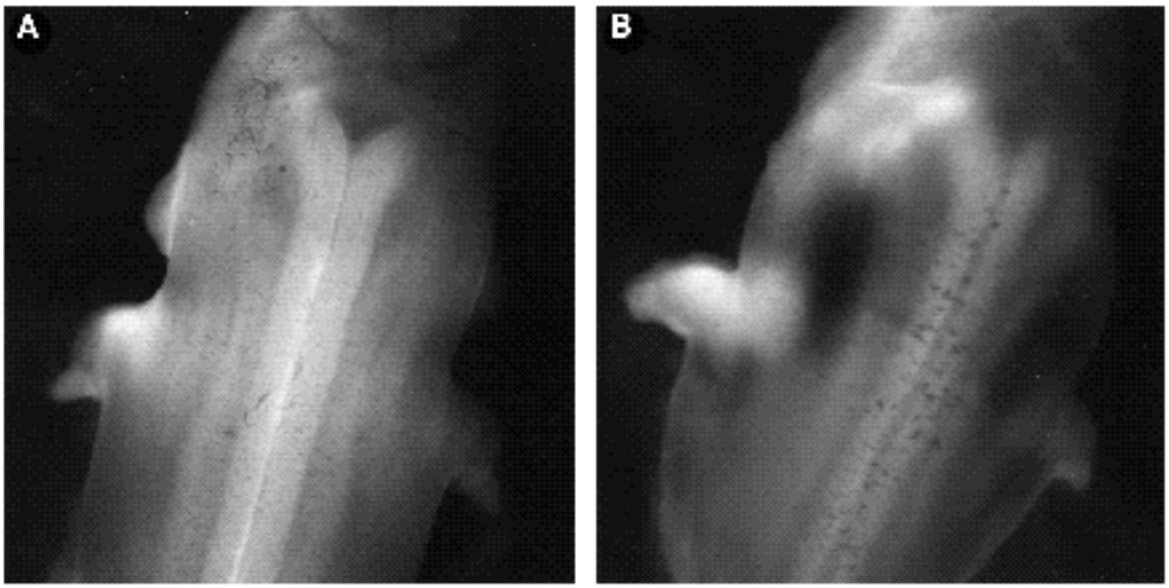


**Fig. 2.** N-*myc*$^{9a/BRP}$ embryos are edematous in the region of the neck. (A) Wild-type 12.5 days p.c. embryo, dorsal view. (B) N-*myc*$^{9a/BRP}$ embryo, showing swelling of the tissue and expanded, blood-filled jugular veins.

side of the N-*myc*$^{9a/BRP}$ embryo (Fig. 5B). The lungs begin their development by budding from the trachea into the surrounding mesenchyme and are visible as two pouches at 10.5 days of development. This early phase of lung development occurred normally in N-*myc*$^{9a/BRP}$ embryos (not shown).

In order to determine whether aspects of lung development other than the branching of the lung epithelium were affected by the reduction in N-Myc protein levels, we performed RNA in situ hybridizations on wild-type and N-*myc*$^{9a/BRP}$ lungs at 12.5 days p.c. (Fig. 6). *Flk-1*, which encodes a tyrosine kinase receptor for vascular endothelial

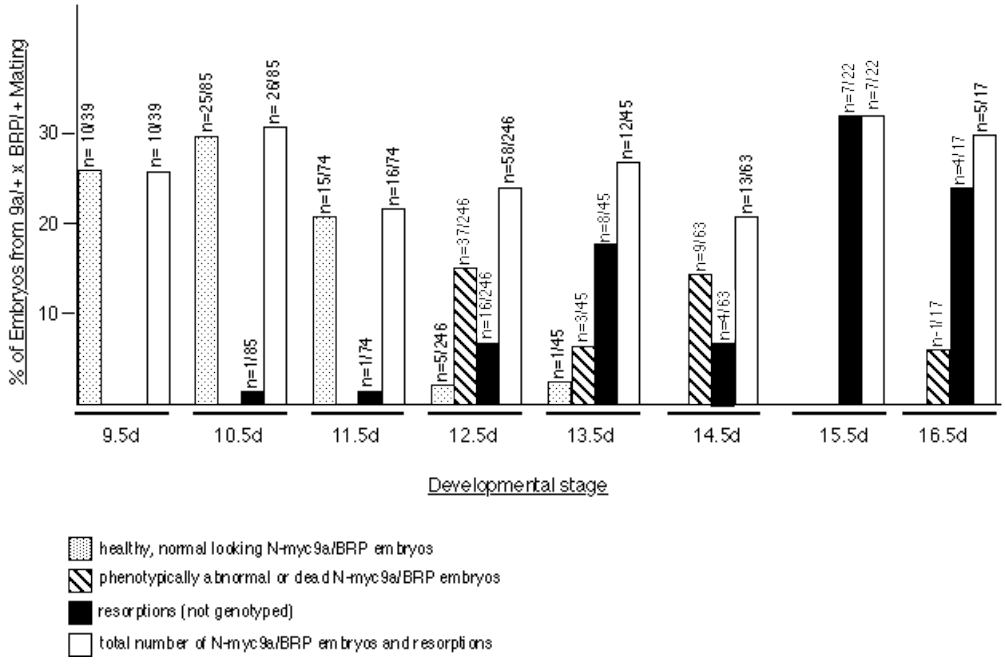


**Fig. 3**. Percentage of embryos in a N-*myc*$^{9a/+}$×N-*myc*$^{BRP/+}$ litter that are N-*myc*$^{9a/BRP}$, as a function of developmental stage. N-*myc*$^{9a/BRP}$ embryos are separated into two groups: (1) healthy, phenotypically normal embryos (stippled bars), and (2) phenotypically abnormal or dead embryos (hatched bars). Resorption sites visible in the uterus but not typed with respect to N-*myc* are included as a separate category (black bars). Note that the total of resorptions, abnormal N-*myc*$^{9a/BRP}$ embryos and normal N-*myc*$^{9a/BRP}$ embryos adds up to approximately 25% of the offspring at each time point (white bars). Numbers are given as a fraction of the total number of embryos dissected from N-*myc*$^{9a/+}$×N-*myc*$^{BRP/+}$ crosses at that developmental stage.

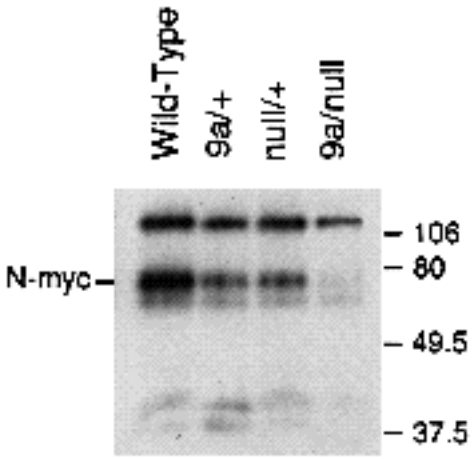


**Fig. 4**. Western analysis of N-Myc protein levels in extracts of 11.5 days p.c. embryos of the four possible types of offspring from an N-*myc*$^{9a/+}$×N-*myc*$^{BRP/+}$ cross. Each lane contains approximately 20 μg of protein. The N-Myc protein runs at approximately 65×10$^3$ $M_r$. A cross-reacting band appears at approximately 100×10$^3$ $M_r$.

growth factor, marks endothelial cells in the developing capillaries and blood vessels in the mouse (Yamaguchi et al., 1993; Millauer et al., 1993), and as such is expressed in a punctate manner throughout the lung mesenchyme where the lung vasculature is developing (Fig. 6C). The pattern and intensity of *flk-1* expression was not affected in N-*myc*$^{9a/BRP}$ lungs (Fig. 6G), indicating that the development of the lung vasculature is not affected by the reduction in N-Myc protein observed in N-*myc*$^{9a/BRP}$ embryos. Fig. 6B,F shows the pattern of expression of N-*myc* in wild-type and N-*myc*$^{9a/BRP}$ lungs, respectively, at 12.5 days p.c., reconfirming that expression is restricted to the lung epithelium and showing that the reduced N-Myc protein levels in N-*myc*$^{9a/BRP}$ embryos did not lead to a complete loss of N-*myc*-expressing cells in the lung epithelium. N-*myc*$^{9a/BRP}$ lungs appeared to express more than 15% of normal levels of N-*myc* RNA (Fig. 6F). This is because the N-*myc*$^{BRP}$ allele encodes a transcript that includes the entire N-*myc* open reading frame, but which contains stop codons that prevent translation of any part of the N-*myc* protein (Stanton et al., 1990). Fig. 6D,H demonstrate that levels of c-*myc* mRNA at the cellular level were not affected by the reduction in N-Myc protein in the lungs of N-*myc*$^{9a/BRP}$ embryos. C-*myc* is normally expressed in the lung mesenchyme (Fig. 6D, Hirning et al., 1991) and the pattern and level of c-*myc* expression was not altered in the N-*myc*$^{9a/BRP}$ lung, despite its reduced size (Fig. 6H).

## Heart development

The other clearly visible defect in N-*myc*$^{9a/BRP}$ embryos examined at 12.5 days p.c. was in the morphology of the heart. While N-*myc*$^{9a/BRP}$ hearts had the normal four-chamber structure, normal endocardial cushions, valves and septa, the heart was small and the myocardium was abnormally thin (Fig. 7A-D). The latter defect was particularly apparent in the 'compact', or subepicardial layer of the ventricular myocardium while the atrial myocardium and the inner trabecular layer of the ventricles were less severely affected. In mammals, trabeculation occurs early during heart development and, at later stages, growth occurs largely in the compact layer (Rumyantsev, 1991). In N-*myc*$^{9a/BRP}$ embryos, this growth of the compact layer appeared not to occur, so that the N-*myc*$^{9a/BRP}$ myocardium at 12.5 days p.c. was no thicker than it had been at 10.5 days p.c.

Occasionally, N-*myc*$^{9a/BRP}$ embryos survived until 14.5 days p.c. These embryos were always grossly abnormal, with large edemas in the neck area, and were smaller than their littermates. Fig. 7E and F compares wild-type and N-*myc*$^{9a/BRP}$ hearts at this stage, showing that the compact layer of the myocardium of the compound heterozygote was still no more developed than it had been at 10.5 days.

It seems likely that this failure in the proliferation of the ventricular myocardium leads to a failure of the circulatory system and ultimately in fetal death. The inefficient function of the heart was demonstrated by the hugely expanded

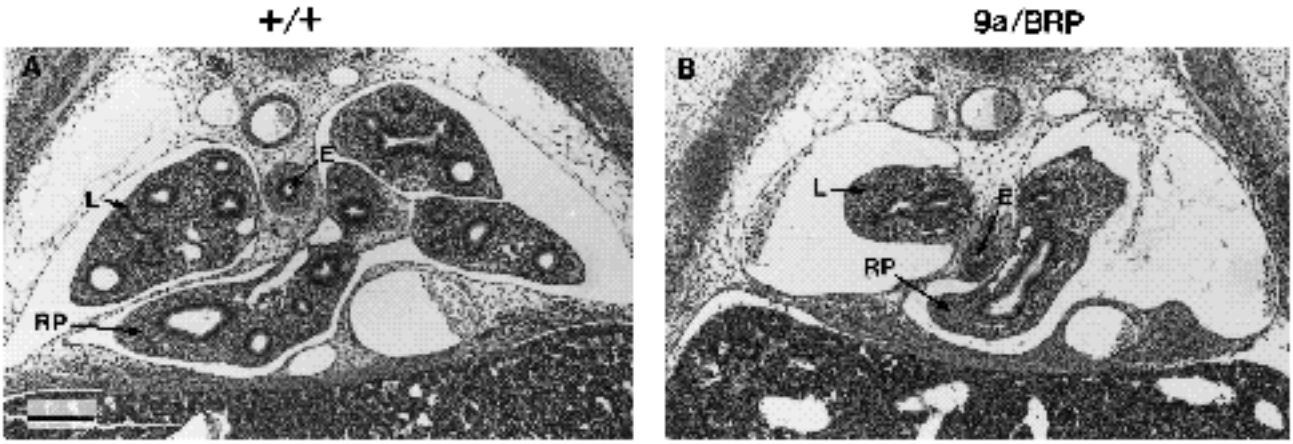


**Fig. 5**. Comparison of lung development in wild-type (A) and compound heterozygote N-*myc*$^{9a/BRP}$ (B) embryos at 12.5 days p.c. Comparable frontal sections were taken at the level of the right postcaval lobe. E, esophagus; L, left lung; RP; right lung, postcaval lobe. Bar, 200 μm.

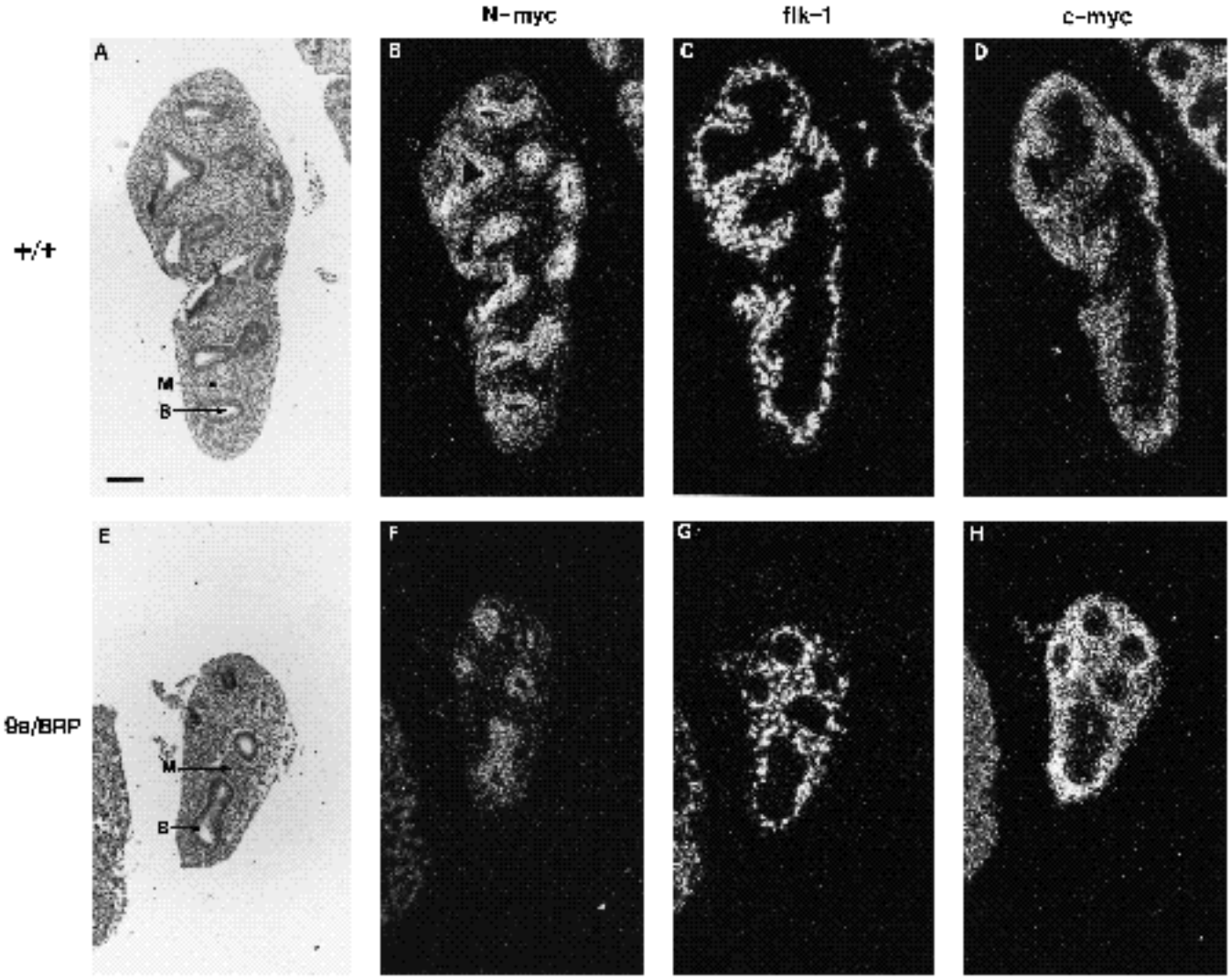


**Fig. 6.** Expression of N-*myc*, *flk-1*, and c-*myc* in wild-type and N-$myc^{9a/BRP}$ lungs at 12.5 days p.c.. (A,E) Bright-field photomicrographs of sagittal sections of the left lung of +/+ (A) and compound heterozygote N-$myc^{9a/BRP}$ (E) embryos. Wild-type (B-D) and N-$myc^{9a/BRP}$ (F-H) serial sections hybridized to the RNA probes shown, were photographed in dark field. B, bronchiole; M, lung mesenchyme. Bar, 100 μm.

jugular veins of N-$myc^{9a/BRP}$ embryos (Fig. 7G,H), since the lack of a highly muscularized ventricular myocardium pumping blood from the heart could lead to a back-up of blood in the major veins. However, it should be noted that we did not see this marked distension in the other major veins that lead into the heart.

We wished to determine whether the observed defect in the development of the compact layer of the ventricular myocardium correlated with N-*myc* expression in the heart. Expression of N-*myc* in the heart at 9.5 days p.c. has been described (Katoh et al., 1991), and we have confirmed this by whole-mount RNA in situ hybridization (data not shown). However the differentiation of trabecular and compact layers has only just begun at this stage, and N-*myc* expression was not shown to be restricted to one specific layer. Our experiments indicate that, by 10.5 days p.c., N-*myc* expression in the heart is largely confined to the compact layer and not to the trabecular layer of the developing ventricular myocardium (Fig. 8B). For comparison, α-cardiac actin, a marker of differentiated myocytes in the developing heart (Sassoon et al., 1988), is expressed in both the trabeculae and the compact layer (Fig. 8C). We observed continued N-*myc* expression in the compact layer at the time when a mutant phenotype was first observed in the heart (12.5 days p.c., Fig. 9B,G). This higher level of of N-*myc* expression in the compact layer compared to the trabecular layer is consistent with a direct role in the development of the mutant phenotype we have observed in N-$myc^{9a/BRP}$ embryos.

Considerable N-*myc* expression was detected in the compact layer of 12.5 days p.c. N-$myc^{9a/BRP}$ hearts (Fig. 9B,G) because the N-$myc^{BRP}$ mutation prevents translation but not transcription of N-*myc*, as noted above. However, as expected, the layer of N-*myc*-expressing cells was narrower in the ventricular myocardium of compound heterozygotes than in the wild-type myocardium (compare Figs 9B and

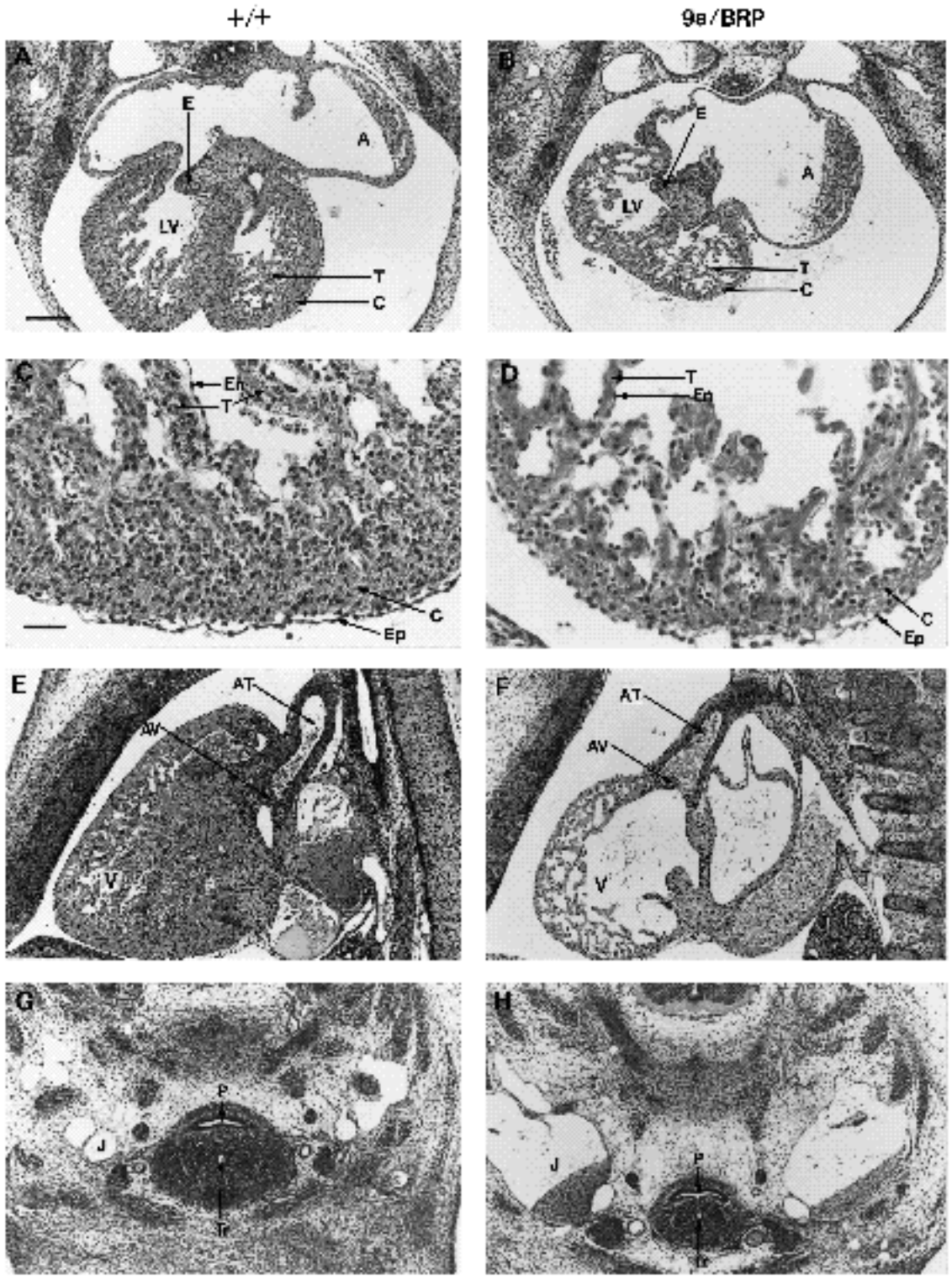


**Fig. 7**. Comparison of heart development in wild-type and compound heterozygote N-*myc*$^{9a/BRP}$ embryos at 12.5 and 14.5 days p.c. Left-hand photographs show wild-type embryos, and right-hand photographs show N-*myc*$^{9a/BRP}$ embryos. (A,B) Low-power magnification photomicrographs of frontal sections of 12.5 days p.c. hearts taken at the level of the left atrioventricular canal. (C,D) High-power magnification of the ventricle of 12.5 day hearts. (E,F) Sagittal sections of 14.5-day hearts. (G,H) Frontal sections through the jugular veins at 12.5 days. A, atrium; AT, aortic trunk; AV, aortic valve; C, compact layer; E, endocardial cushion; En, endocardium; Ep, epicardium; J, jugular veins; LV, left ventricle; P, pharynx; V, ventricle; T, trabeculae; Tr, trachea. For A,B,E,F,G,H: bar, 250 μm; for C,D: bar, 50 μm.

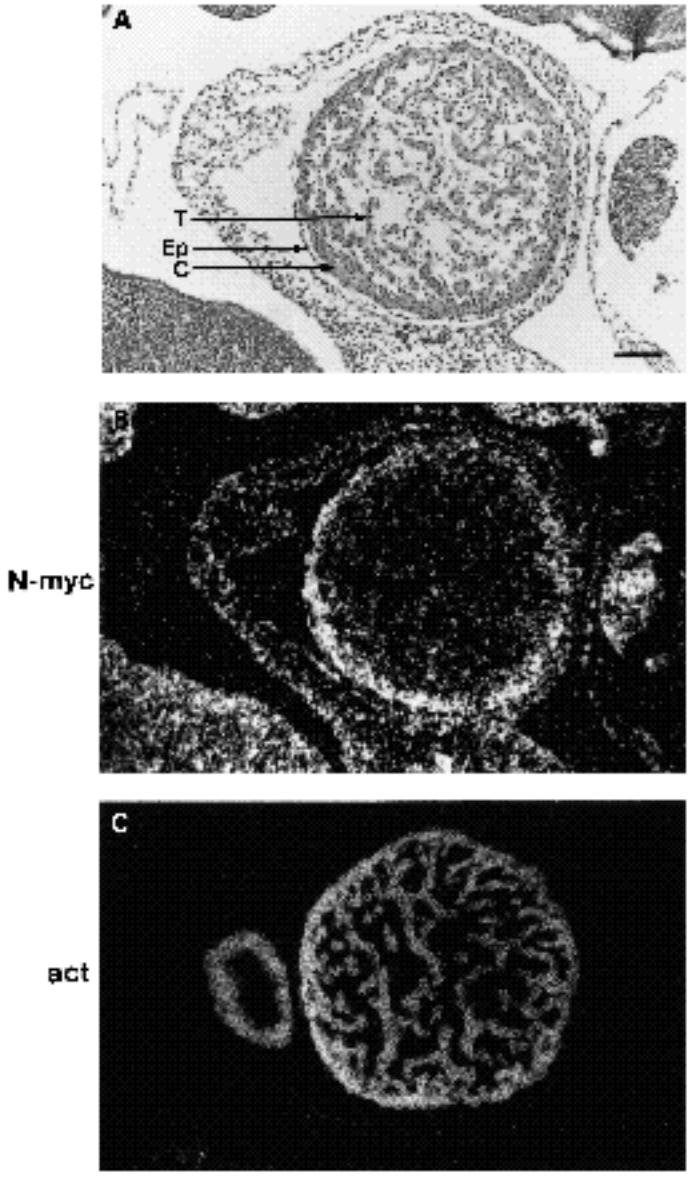


**Fig. 8.** Expression patterns of N-*myc* and α-cardiac actin in the heart at 10.5 days p.c. (A) Bright-field photomicrograph of a hematoxylin and eosin-stained parasagittal section of a wild-type ventricle. (B,C) Dark-field photomicrographs of serial sections showing N-*myc* (B) and α-cardiac actin (C) expression by RNA in situ hybridization. C, compact subepicardial layer; T, trabeculae; Ep, epicardium. Bar, 100 μm.

8B). The observation that the mutant alleles continue to be transcribed in the N-$myc^{9a/BRP}$ myocardium suggests that cells that normally express N-*myc* are present but in reduced numbers.

*Flk-1*, the endothelial cell marker described above, is expressed in the endocardium (Yamaguchi et al., 1993), which is the mesodermally derived inner lining of the heart that later contributes to the endocardial cushion and heart valves through an epithelial-to-mesenchymal transition (Fig. 9D,I; Markwald et al., 1990). The differentiation of the endocardium was not affected in N-$myc^{9a/BRP}$ embryos, as demonstrated by the continued expression of *flk-1* in the endocardium (compare Figs 10D,I and 8D,I). The N-$myc^{9a/BRP}$ genotype also did not prevent the differentiation of cardiac myocytes in the myocardium, as indicated by the strong expression of α-cardiac actin in both the compact and trabecular layers of the mutant myocardium (compare Figs 10C,H and 9C,H).

The finding that reduction in N-*myc* expression in the compact layer of the heart caused a myocyte hypoplasia evident at 12.5 days p.c. was interesting, in that overexpression of the closely related c-*myc* proto-oncogene in the heart of transgenic mice has been described to cause a hyperplasia of the myocytes which is also evident during development (Jackson et al., 1990). The normal expression pattern of c-*myc* in the heart has not been described, so the relative roles of these two genes in myocyte proliferation in vivo was not clear. Fig. 9E,J demonstrates that c-*myc* is expressed at low levels in the heart, and that its pattern of expression is different, and to some extent complementary to that of N-*myc*. While N-*myc* is expressed in the compact layer of the ventricular myocardium, c-*myc* expression is largely restricted to cells adjacent to and on the outside of the compact layer, and to isolated cells or clusters of cells adjacent to and on the inside of the compact layer. The expression on the outer surface of the heart is similar to that of *flk-1* (Fig. 8D,I) and probably represents expression in the capillaries that run between the myocardium and epicardium (Viragh and Challice, 1981). The small foci of grains on the inner surface of the myocardium also appears to represent c-*myc* expression in endocardial cells, as they are found specifically in the vicinity of red-blood-cell-containing capillaries. c-*myc* mRNA was also observed in endothelial cells lining the endocardial cushion. c-*myc* is only expressed at low levels in the myocardium itself, in spite of the fact that when it is expressed ectopically in the myocardium it causes myocytic hyperplasia (Jackson et al., 1990). In N-$myc^{9a/BRP}$ hearts, the expression of c-*myc* did not appear to be affected (Fig. 10E,J).

### Other tissues

Careful examination of N-$myc^{9a/BRP}$ embryos between 10.5 and 14.5 days p.c. gave no evidence of defects in the kidney or brain, both of which are major sites of N-*myc* expression in the embryo, and both of which are affected in N-$myc^{BRP/BRP}$ embryos (Stanton et al., 1992; Charron et al., 1992). In four N-$myc^{9a/BRP}$ embryos that survived until 14.5 days p.c., the kidneys were small but were structurally normal (not shown). N-$myc^{BRP/BRP}$ mice have also been described as having reduced genital ridges (Stanton et al., 1992) and cranial and spinal ganglia. However, these structures were indistinguishable in N-$myc^{9a/BRP}$ embryos from those of their wild-type littermates (not shown).

## DISCUSSION

We have generated mice that carry two different mutant alleles of the N-*myc* proto-oncogene in order to identify functions for N-*myc* that were not revealed in mice homozygous for each mutation individually. The N-$myc^{9a}$ allele is a leaky mutation which in the homozygous condition causes perinatal lethality due to a defect early in lung branching

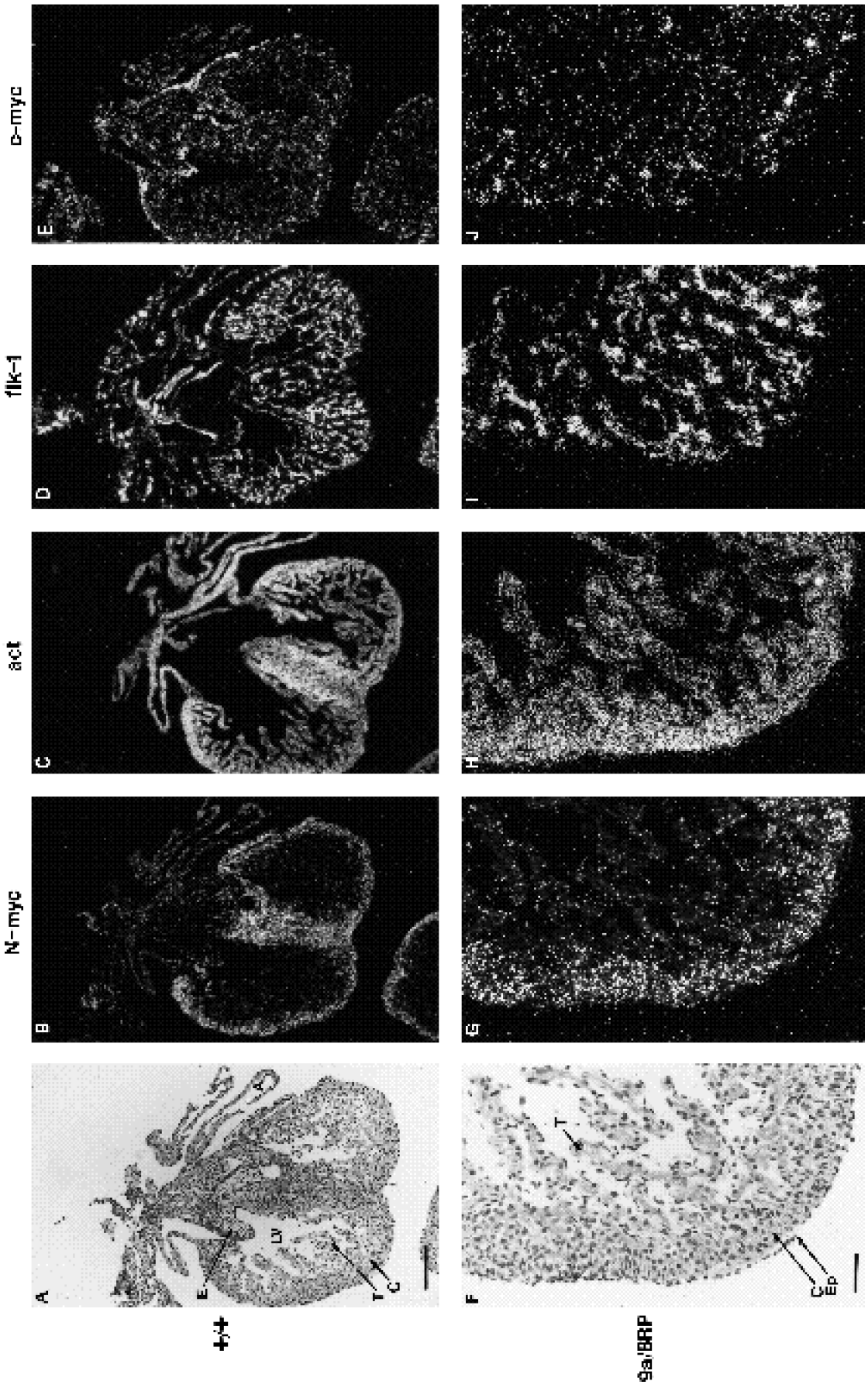


**Fig. 9.** Expression of N-*myc*, α-cardiac actin, *flk-1* and c-*myc* in the wild-type heart at 12.5 days p.c. (A) Bright-field photomicrograph of a hematoxylin and eosin-stained frontal section in the region of the left atrioventricular canal. (F) High power magnification of the section shown in a, through the ventricle. (B-E) Dark-field photomicrographs of serial sections hybridized to the RNA probes shown above. (G-J) High power detail of the sections shown in B-E. Act, α-cardiac actin; A, atrium; C, compact layer; E, endocardial cushion; Ep, epicardium; LV, left ventricle; T, trabeculae. For A-E, bar, 200 μm; for F-J, bar, 50 μm.

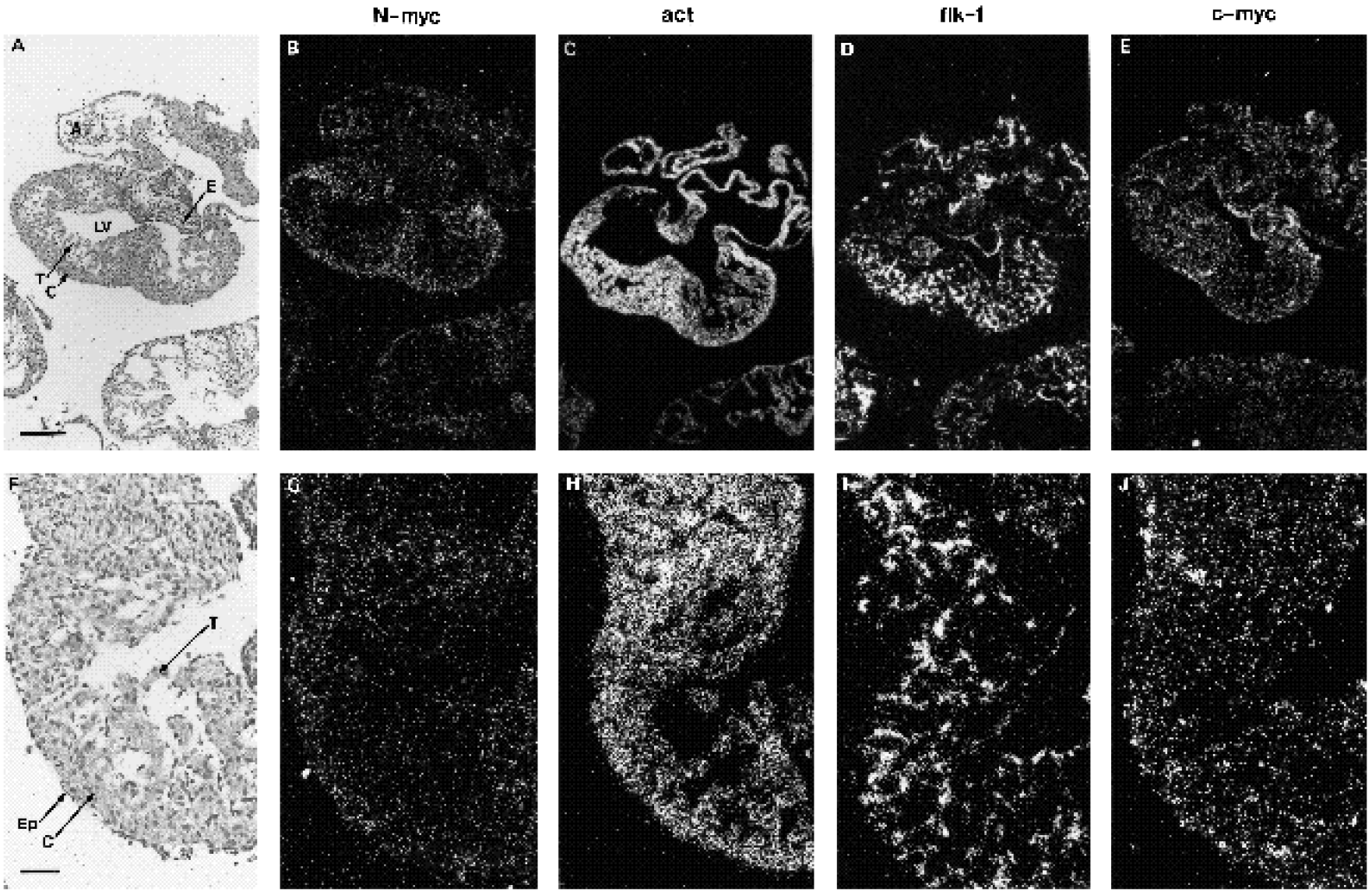


**Fig. 10**. Expression of N-*myc*, α-cardiac actin, *flk-1* and c-*myc* in compound heterozygote N-*myc*$^{9a/BRP}$ heart at 12.5 days p.c. (A) Bright-field photomicrograph of a hematoxylin and eosin-stained frontal section in a region comparable to that shown in Fig. 9. (F) High power magnification of the section shown in A, through the ventricle. (B-E) Dark-field photomicrographs of serial sections hybridized to the RNA probes shown. (G-J) High power detail of the sections shown in B-E. Act, α-cardiac actin; A, atrium; C, compact layer; E, endocardial cushion; Ep, epicardium; LV, left ventricle; T, trabeculae. For A-E, bar, 200 μm, for F-J, bar, 50 μm

morphogenesis. The levels of residual N-Myc protein (approximately 25% of normal levels) are presumably sufficient to support the normal development of other tissues in which N-*myc* normally functions. The N-*myc*$^{BRP}$ allele is likely to be a mutation which, in the homozygous condition, results in embryonic lethality at approximately 11.5 days p.c., at which point the epithelial component of the mesonephros, brain, lung, stomach and intestine are all hypoplastic (Stanton et al., 1992). The phenotype of N-*myc*$^{9a/BRP}$ compound heterozygotes is intermediate to the two homozygous mutant phenotypes, consistent with the observation that the N-*myc*$^{9a/BRP}$ heterozygotes contain lower levels of N-Myc protein than are present in N-*myc*$^{9a/9a}$ embryos. N-*myc*$^{9a/BRP}$ embryos die between 12 and 15 days p.c., and a number of tissues that are affected in N-*myc*$^{BRP/BRP}$ homozygotes, such as the kidney, brain and cranial and spinal sensory ganglia, appear to be normal. The lungs, which are the main organ affected in N-*myc*$^{9a/9a}$ homozygotes, are even more severely affected in N-*myc*$^{9a/BRP}$ embryos. Compound heterozygotes also showed a defect in the development of the compact subepicardial layer of the heart, and appeared to die from a failure of heart function caused by a hypoplasia of ventricular myocytes in the compact layer. These results indicate a critical role for N-*myc* in the development of the heart.

### N-*myc* in heart development

The reduced levels of N-Myc protein found in N-*myc*$^{9a/BRP}$ embryos result in a considerable thinning of the subepicardial compact layer of the myocardium by 12.5 days of development. Consistent with this phenotype, N-*myc* expression is expressed much more strongly in the compact layer of the heart at 10.5 and 12.5 days p.c. than in the trabecular layer of the myocardium or in the endothelium. Trabeculation, or formation of the myocardial projections that form a lattice of contractile cells throughout much of the ventricles of the embryonic heart, occurs early during heart development in the mouse, beginning around day 9.5 of gestation (Challice and Viragh, 1973). By a number of ultrastructural and cytochemical criteria, the myocytes within the trabeculae are more highly differentiated than the myocytes in the compact layer (Rumyantsev, 1991). Thus compact layer myocytes are more basophilic and richer in RNA, while trabecular myocytes contain more mitochondria, ribosomes and granular endoplasmic reticulum. Myofibrils in trabecular myocytes are thicker and more highly organized than in compact layer myocytes, where myofibrils are present but are scattered randomly relative to one another in the cytoplasm. Consistent with this picture is the observation that the rate of cell proliferation in the compact layer is 2- to 3-fold higher than in the trabeculae (Rumyantsev, 1977; Tokuyasu, 1990). The highly differentiated myocytes in the trabecular layer have been postulated to be responsible for the early beating of the heart while, at later stages, the thickened compact layer becomes the major contractile force. The cardiac hypoplasia that we observe in N-*myc*$^{9a/BRP}$ embryos is more apparent in the compact layer. This may explain our observation that embryonic lethality does not occur until later during heart development, when heart function may depend more on the compact layer than on the trabecular layer.

Our observation of N-*myc* expression in the compact layer and the absence of development in the compact layer in N-*myc*$^{9a/BRP}$ mice suggests that N-*myc* is required either for the proliferation of myocytes in the compact layer, and/or for preventing the differentiation of these cells, although there are other possible explanations, such as that they are dying prematurely. The simplest explanation is the former. However, the second hypothesis, in which N-*myc* expression prevents the terminal differentiation of compact layer myocytes into trabecular-type myocytes, is consistent with previous descriptions of N-*myc* expression in the embryo, in which N-*myc* expression is correlated with cells in an undifferentiated state in the kidney, brain and skin, regardless of their proliferative state, and the further differentiation of these cells is correlated with down-regulation of N-*myc* (Mugrauer et al., 1988).

In their description of embryos homozygous for a null mutation in N-*myc*, Charron et al. (1992) noted a defect in the development in the heart, visible as early as 9.5 days p.c., in which development was apparently slowed as evidenced by the absence of endocardial cushion tissue and of interatrial and interventricular septa. It was postulated that N-*myc* is involved in the generation of the inductive signal sent by the myocardium to the endocardium to induce the epithelial-to-mesenchymal transition of the endocardium, which forms these anlagen of the cardiac valves and septa. Our results confirm a function for N-*myc* in the development in the heart, but tend to support a role for N-*myc* within the myocardium itself, although this could presumably have a secondary impact on endocardial differentiation in more severe mutants. We have not observed defects in the formation of septal or endocardial cushion tissue in N-*myc*$^{9a/BRP}$ embryos.

### c-*myc* in heart development

When c-*myc* is overexpressed in the heart of RSV/c-*myc* transgenic mice, these mice develop a fetal cardiac myocyte hyperplasia and at birth have more than twice the normal number of cardiac myocytes (Jackson et al., 1990). This has suggested that endogenous c-*myc* may play a role in cardiac myocyte proliferation in vivo. However, we have demonstrated that c-*myc* is only expressed at low levels in the heart at 12.5 days p.c. and that this expression is largely in endothelial cells and not in the myocardium. Background levels of c-*myc* expression in the heart were also observed in mouse embryos at 13.5 days p.c. (Stanton et al., 1992) and in first trimester human embryos (Pfeifer-Ohlsson et al., 1985). N-*myc*, in contrast, is expressed at high levels in the compact layer of the ventricular myocardium at 10.5 and 12.5 days. Combined with the hypoplasia of the myocardium that we have observed in N-*myc*$^{9a/BRP}$ embryos, these data suggest that N-*myc* rather than c-*myc* may play a primary role in the regulation of proliferation and/or differentiation of ventricular myocytes during heart development, and that the effect of c-*myc* in these transgenic mice may reflect the possibility that in this instance c-*myc* can mimic the normal effects of N-*myc*. It has previously been observed that different *myc* family genes can cause the same tumour types in transgenic mice when they are overexpressed using identical promoters, even though this expression may be ectopic (Rosenbaum et al., 1989; Dildrop

et al., 1989; Adams et al., 1985). Furthermore, high levels of expression of one *myc* gene in transgenic mice can repress transcription of itself and of other *myc* genes (Rosenbaum et al., 1989; Dildrop et al., 1989; Adams et al., 1985). These results have suggested that at high levels, the various *myc* genes may be able to mimic each other's effects on downstream targets. This hypothesis has been strengthened by the observations that N-Myc and c-Myc proteins bind the same core DNA sequence in vitro, and that N-, L- and c-*myc* all form heterodimers with Max in vivo (Blackwood et al., 1992; Wenzel et al., 1991; Mukherjee et al., 1992), and all transform cells in culture through their interaction with Max (Mukherjee et al., 1992). We are presently crossing RSV/c-*myc* mice with the N-*myc* mutant mice to generate N-$myc^{9a/BRP}$ embryos that also express this c-*myc* transgene in the heart. If c-*myc* in these transgenics truly mimicks the normal role of N-*myc*, the cardiac myocyte hypoplasia of compound heterozygous embryos is expected to be rescued by the transgene.

Recently, Davis et al. (1993) have described the phenotype of mice that bear a null mutation in c-*myc*. These embryos die before 10.5 days p.c. and exhibit, among other abnormalities, an enlargement of the heart and a dilated, fluid-filled pericardium. This is unexpected in light of the observation, described above, that mice with ectopic expression of c-*myc* in the heart have enlarged hearts. However, it is still unclear whether the heart abnormality in the c-*myc* null mutants is a direct result of the mutation or is secondary to other defects that are causing the embryo to die.

In spite of the possibility that c-*myc* expression may be able to replace N-*myc* function, we observe no up-regulation of c-*myc* in either the compact layer of the myocardium or in the lung epithelium of N-$myc^{9a/BRP}$ mice. This may be because cross-regulation of the *myc* family genes does not normally occur in these tissues as it does when they are overexpressed in transformed cells or in transgenic mice. Stanton et al. (1992) showed that c-*myc* is expressed in the telencephalon of N-$myc^{BRP/BRP}$ embryos, and this observation was interpreted to indicate cross regulation of N-*myc* and c-*myc* in the neuroepithelium.

## N-*myc* in lung development

Mice homozygous for the N-$myc^{9a}$ mutation die at birth due to a defect in lung morphogenesis which is visible as early as 12.5 days p.c. (Moens et al., 1992). We have postulated that N-*myc* is required for the lung epithelium to respond to local inductive signals emanating from the lung mesenchyme, which cause branching to occur. N-$myc^{9a/BRP}$ embryos have more severely affected lungs, with only a rudimentary branching pattern at 12.5 days. However, the earliest events of lung development, in which two buds are induced to grow from the trachea by surrounding mesenchyme (Spooner and Wessells, 1970), occur normally in N-$myc^{9a/BRP}$ and indeed in N-$myc^{BRP/BRP}$ embryos (Stanton et al., 1992). We and others (Hirning et al., 1991; Moens et al., 1992) have shown that N-*myc* is expressed in the lung epithelium and, further, that expression is largely restricted to bronchioles and is present at very low levels in the trachea and bronchi. These results suggest that N-*myc* is involved in branching morphogenesis in the lung but not in the initial induction of budding of the tracheal epithelium. Experimental manipulations in vitro have suggested that there are different mechanisms for budding versus branching of the lung epithelium. A number of different stimuli, including salivary gland mesenchyme and bronchial mesenchyme, can induce supernumerary buds in tracheal epithelium, but only bronchial mesenchyme is able to induce those buds to branch (Wessells, 1970; Spooner and Wessells, 1970). The phenotypes of mice bearing mutations in N-*myc* provide genetic evidence for such a mechanism for lung development and provide a candidate gene that is involved in the control of one process (branching) and not the other (budding).

## Tissue-specific effects of N-myc mutant alleles

Only a subset of the tissues that normally express N-*myc* are visibly affected in N-$myc^{9a/BRP}$ embryos. N-$myc^{9a/9a}$ embryos have approximately 25% of wild-type levels of N-Myc protein and, in these embryos, the lungs and spleen are the only tissues affected (Moens et al., 1992). N-$myc^{9a/BRP}$ embryos have approximately 15% of wild-type levels of N-Myc protein and, in these embryos, the heart is also affected. However, 15% of normal levels of N-Myc protein appear to be sufficient for normal genitourinary and nervous system development. The molecular basis for this remains to be determined. It is possible that different tissues within the embryo make different amounts of normal protein relative to the amounts in wild-type embryos. We have previously attempted to correlate the relative levels of normal N-*myc* mRNA in different tissues of N-$myc^{9a/9a}$ embryos with the presence or absence of a mutant phenotype (Moens et al., 1992) and, although there were differences among the tissues examined, no strong correlation could be established. Another explanation for the tissue-specific effects of N-*myc* mutant alleles is that different tissues are affected differently by approximately the same reduction in N-Myc protein because of differences in the ratio of N-Myc protein to Max (Blackwood and Eisenman, 1991), to Max-associated proteins such as Mad and Mxi1 (Ayer et al., 1993; Zervos et al., 1993), or to other Myc proteins.

Myc proteins require dimerization with Max for DNA binding (Blackwood and Eisenman, 1991; Prendergast and Ziff, 1991; Kato et al., 1992). A number of lines of evidence have suggested that Max overexpression can inhibit transformation (Mukherjee et al., 1992; Makela et al., 1992; Prendergast et al., 1992) and transactivation (Kretzner et al., 1992; Amati et al., 1992) by *myc* genes. Mad, cloned by virtue of its ability to dimerize with Max, has been shown to compete with Myc for binding to Max, and to thereby inhibit transactivation by Myc (Ayer et al., 1993). Mxi1 (Zervos et al., 1993) and other, as yet unidentified, Max partners presumably act in a similar manner and are also likely thereby to inhibit N-*myc* function. Also, L-Myc, a poorly transforming member of the Myc family, has been shown to prevent transformation by other *myc* genes, presumably by competing for and forming less active DNA-bound complexes with Max (Mukherjee et al., 1992). In cell types where a number of Max-associated and Myc proteins compete with N-Myc protein for dimerization with Max and sites on DNA, an 85% reduction in N-Myc protein is expected to reduce the response of downstream targets of N-

Myc more strongly than in cells where there are no competitors for Max binding. Interestingly, L-*myc* is co-expressed with N-*myc* in the lung, perhaps in the same cell type (Zimmerman et al., 1986), but the two genes are not co-expressed in the kidney (Mugrauer and Ekblom, 1991), where neither the N-*myc*$^{9a/9a}$ nor the N-*myc*$^{9a/BRP}$ embryos have an abnormal phenotype. It will be interesting to compare the detailed expression patterns of the various interacting factors with the tissues affected by the N-*myc* mutations.

## Conclusions

We have generated a third N-*myc* mutant phenotype by combining leaky and null alleles in a compound heterozygote. These mice have allowed us to study the function of N-*myc* at a stage in development that is not reached in embryos homozygous for the null allele (Stanton et al., 1992) and that is not affected in embryos homozygous for the leaky allele (Moens et al., 1992). Classical genetic studies of development in a number of systems have demonstrated the importance of studying the phenotypic effects of different mutant alleles and combinations of mutant alleles in a given gene in order to determine its multiple roles in the course of development. Our results have shown that the technique of gene targeting by homologous recombination in the mouse can be used to the same ends. The clear delineation of a function for N-*myc* in both lung branching morphogenesis and myocardial development also provides target tissues in which to search for the elusive downstream genes in the N-*myc* signaling pathway.

## Note added after acceptance

Recently, a third description of embryos homozygous for a putative null allele of N-*myc* has been published (Sawai et al., 1993). The overall phenotype of these mutant embryos is very similar to those described by Stanton et al. (1992) and Charron et al. (1992), but the defect in heart development is shown to be primarily in the myocardium.

We wish to thank Dr R. Kennett for the anti-N-*myc* antibody, Dr M. Buckingham for the α-cardiac actin probe, T. Yamaguchi for the *flk-1* probe, Dr C. Asselin for the c-*myc* probe and Dr R. DePinho for the N-*myc* genomic clone from which probes for RNA in situ hybridization were subcloned. Our gratitude also to Dr Arch Perkins for his help in the phenotypic analysis of N-*myc*$^{9a/BRP}$ mutants, to Alexandra Joyner for her critical reading of the manuscript, and to Valerie Prideaux, Chi-Chong Hui, Benny Motro and Ester Ivanyi for their generous assistance in various aspects of this work. This work was supported by a Terry Fox program project grant from the National Cancer Institute of Canada. C. B. M. was supported by a Natural Sciences and Engineering Research Council of Canada 'Centennial' Scholarship and a Medical Research Council of Canada Studentship. J. R. is an International Scholar of the Howard Hughes Medical Institute and a Terry Fox Cancer Research Scientist of the National Cancer Institute of Canada. B. R. S. and L. F. P. are sponsored by the NCI-DHHS under contract NO1-CO-74101 with ABL.

## REFERENCES

**Adams, J. M., Harris, A. W., Pinkert, C. A., Corcoran, L. M., Alexander, W. S., Cory, S., Palmiter, R. D. and Brinster, R. L.** (1985). The c-myc oncogene driven by immunoglobulin enhancers induces lymphoid malignancy in transgenic mice. *Nature* **318**, 533-538.

**Alex, R., Soezeri, O., Meyer, S. and Dildrop, R.** (1992). Determination of the DNA sequence recognized by the bHLH-zip domain of the N-Myc protein. *Nucleic Acids Res.* **20**, 2257-2263.

**Amati, B., Dalton, S., Brooks, M. W., Littlewood, T. D., Evan, G. I. and Land, H.** (1992). Transcriptional activation by the human c-Myc oncoprotein in yeast requires interaction with Max. *Nature* **359**, 423-426.

**Amati, B., Brooks, M. W., Levy, N., Littlewood, T. D., Evan, G. I. and Land, H.** (1993). Oncogenic activity of the c-Myc protein requires dimerization with Max. *Cell* **72**, 233-245.

**Ayer, D. E., Kretzner, L. and Eisenman, R. N.** (1993). Mad: a heterodimeric partner for Max that antagonizes Myc transcriptional activity. *Cell* **72**, 211-222.

**Barrett, J., Birrer, M. J., Kato, G. J., Dosaka-Akita, H. and Dang, C. V.** (1992). Activation domains of L-Myc and c-Myc determine their transforming potencies in rat embryo cells. *Mol. Cell Biol.* **12**, 3130-3137.

**Blackwell, T. K., Kretzner, L., Blackwood, E. M., Eisenman, R. N. and Weintraub, H.** (1990). Sequence-specific DNA binding by the c-Myc protein. *Science* **250**, 1149-1151.

**Blackwood, E. M., Luescher, B. and Eisenman, R. N.** (1992). Myc and Max associate in vivo. *Genes Dev.* **6**, 71-80.

**Blackwood, E. M. and Eisenman, R. N.** (1991). Max: a helix-loop-helix zipper protein that forms a sequence-specific DNA-binding complex with Myc. *Science* **251**, 1211-1217.

**Bossone, S. A., Asselin, C., Patel, A. J. and Marcu, K. B.** (1992). Maz, a zinc finger protein, binds to c-MYC and C2 gene sequences regulating transcriptional initiation and termination. *Proc. Natl. Acad. Sci. USA* **89**, 7452-7456.

**Challice, C. E. and Viragh, S.** (1973). The architectural development of the early mammalian heart. *Tissue Cell* **6**, 447-462.

**Charron, J., Malynn, B. A., Robertson, E. J., Goff, S. P. and Alt, F. W.** (1990). High-frequency disruption of the N-myc gene in embryonic stem and pre-B cell lines by homologous recombination. *Mol. Cell Biol.* **10**, 1799-1804.

**Charron, J., Malynn, B. A., Fisher, P., Stewart, V., Jeannotte, L., Goff, S. P., Robertson, E. J. and Alt, F. W.** (1992). Embryonic lethality in mice homozygous for a targeted disruption of the N-myc gene. *Genes Dev.* **6**, 2248-2257.

**Davis, A. C., Wims, M., Spotts, G. D., Hann, S. R. and Bradley, A.** (1993). A null c-*myc* mutation causes lethality before 10.5 days of gestation in homozygotes and reduced fertility in heterozygous female mice. *Genes Dev.* **7**, 671-682.

**DePinho, R. A., Legouy, E., Feldman, L. B., Kohl, N. E., Yancopoulos, G. D. and Alt, F. W.** (1986). Structure and expression of the murine N-myc gene. *Proc. Natl. Acad. Sci. USA* **83**, 1827-1831.

**DePinho, R. A., Schreiber-Agus, N. and Alt, F. W.** (1991). myc family oncogenes in the development of normal and neoplastic cells. *Adv. Cancer Res.* **57**, 1-46.

**Dildrop, R., Ma, A., Zimmerman, K., Hsu, E., Tesfaye, A., DePinho, R. A. and Alt, F. W.** (1989). IgH enhancer-mediated deregulation of N-myc gene expression in transgenic mice: generation of lymphoid neoplasias that lack c-myc expression. *EMBO J.* **8**, 1121-1128.

**Frohman, M. A., Boyle, M. and Martin, G. R.** (1990). Isolation of the mouse Hox-2.9 gene; Analysis of embryonic expression suggests that positional information along the anterior-posterior axis is specified by mesoderm. *Development* **110**, 589-607.

**Garrell, J. and Campuzano, S.** (1991). The helix-loop-helix domain: A common motif for bristles, muscles and sex. *BioEssays* **13**, 493-498.

**Hirning, U., Schmid, P., Schulz, W. A., Rettenberger, G. and Hameister, H.** (1991). A comparative analysis of N-myc and c-myc expression and cellular proliferation in mouse organogenesis. *Mech. Dev.* **33**, 119-126.

**Ikegaki, N., Bukovsky, J. and Kennett, R. H.** (1986). Identification and characterization of the NMYC gene product in human neuroblastoma cells by monoclonal antibodies with defined specificities. *Proc. Natl. Acad. Sci. USA* **83**, 5929-5933.

**Ikegaki, N. and Kennett, R. H.** (1989). Glutaraldehyde fixation of the primary antibody-antigen complex on nitrocellulose paper increases the overall sensitivity of immunoblot assay. *J. Immunol. Met.* **124,** 205-210.

**Jackson, T., Allard, M. F., Sreenan, C. M., Doss, L. K., Bishop, S. P. and Swain, J. L.** (1990). The c-myc proto-oncogene regulates cardiac development in transgenic mice. *Mol. Cell Biol.* **10**, 3709-3716.

**Kato, G. J., Barrett, J., Villa-Garcia, M. and Dang, C. V.** (1990). An

amino-terminal c-Myc domain required for neoplastic transformation activates transcription. *Mol. Cell Biol.* **10**, 5914-5920.

**Kato, G. J., Lee, W. M. F., Chen, L. and Dang, C. V.** (1992). Max: Functional domains and interaction with c-Myc. *Genes Dev.* **6**, 81-92.

**Katoh, K., Kanamori, A., Wakamatsu, Y., Sawai, S. and Kondoh, H.** (1991). Tissue distribution of N-myc expression in the early organogenesis period of the mouse embryo. *Dev. Growth Diff.* **33**, 29-36.

**Kohl, N. E., Kanda, N., Schrenck, R. R., Bruns, G., Latt, S. A., Gilbert, F. and Alt, F. W.** (1983). Transposition and amplification of oncogene-related sequences in human neuroblastomas. *Cell* **35**, 359-367.

**Kretzner, L., Blackwood, E. M. and Eisenman, R. N.** (1992). Myc and Max proteins possess distinct transcriptional activities. *Nature* **359**, 426-429.

**Lee, W. H., Murphree, A. L. and Benedict, W. F.** (1984). Expression and amplification of the N-myc gene in primary retinoblastoma. *Nature* **309**, 458-460.

**Makela, T. P., Koskinen, P. J., Vastrik, I. and Alitalo, K.** (1992). Alternative forms of Max as enhancers or suppressors of Myc-Ras cotransformation. *Science* **256**, 373-377.

**Markwald, R. R., Mjaatvedt, C. H., Krug, E. L. and Sinning, A. R.** (1990). Inductive interactions in heart development: role of cardiac adherons in cushion tissue formation. *Ann. NY Acad. Sci.* **588**, 13-25.

**Millauer, B., Wizigmann-Voos, S., Schnurch, H., Martinez, R., Moller, N. P. H., Risau, W. and Ullrich, A.** (1993). High affinity VEGF binding and developmental expression suggest Flk-1 as a major regulator of vasculogenesis and angiogenesis. *Cell* **72,** 835-846.

**Moens, C. Bernelot, Auerbach, A. B., Conlon, R. A., Joyner, A. L. and Rossant, J.** (1992). A targeted mutation reveals a role for N-myc in branching morphogenesis in the embryonic mouse lung. *Genes Dev*. **6**, 691-704.

**Mugrauer, G., Alt, F. W. and Ekblom, P.** (1988). N-myc proto-oncogene expression during organogenesis in the developing mouse as revealed by in situ hybridization. *J. Cell Biol.* **107**, 1325-1335.

**Mugrauer, G. and Ekblom, P.** (1991). Contrasting expression patterns of three members of the myc family of protooncogenes in the developing and adult mouse kidney. *J. Cell Biol.* **112**, 13-25.

**Mukherjee, B., Morgenbesser, S. D. and DePinho, R. A.** (1992). Myc family oncoproteins function through a common pathway to transform normal cells in culture: cross-interference by Max and trans-acting dominant mutants. *Genes Dev.* **6**, 1480-1492.

**Nau, M. M., Brooks, B. J., Jr., Carney, D. N., Gazdar, A. F., Battey, J. F., Sausville, E. A. and Minna, J. D.** (1986). Human small-cell lung cancers show amplification and expression of the N-myc gene. *Proc. Natl. Acad. Sci. USA* **83**, 1092-1096.

**Nisen, P. D., Zimmerman, K., Cotter, S. V., Gilbert, F. and Alt, F. W.** (1986). Enhanced expression of the N-myc gene in Wilms' tumours. *Cancer Res.* **46**, 6217-6222.

**Pfeifer-Ohlsson, S., Rydnert, J., Goustin, A. S., Larsson, E., Betsholtz, C. and Ohlsson, R.** (1985). Cell-type-specific pattern of myc protooncogene expression in developing human embryos. *Proc. Natl. Acad. Sci. USA* **82**, 5050-5054.

**Prendergast, G. C., Lawe, D. and Ziff, E. B.** (1991). Association of Myn, the murine homolog of Max, with c-Myc stimulates methylation-sensitive DNA binding and Ras cotransformation. *Cell* **65,** 395-407.

**Prendergast, G. C., Hopewell, R., Gorham, B. J. and Ziff, E. B.** (1992). Biphasic effect of Max on Myc cotransformation activity and dependence on amino- and carboxy-terminal Max functions. *Genes Dev.* **6**, 2429-2439.

**Prendergast, G. C. and Ziff, E. B.** (1991). Methylation-sensitive sequence-specific DNA binding by the c-myc basic region. *Science* **251**, 186-189.

**Resar, L. M. S., Dolde, C., Barrett, J. F. and Dang, C. V.** (1993). B-myc inhibits neoplastic transformation and transcriptional activation by c-myc. *Mol. Cell Biol.* **13**, 1130-1136.

**Rosenbaum, H., Webb, E., Adams, J. M., Cory, S. and Harris, A. W.** (1989). N-myc transgene promotes B lymphoid proliferation, elicits lymphomas and reveals cross-regulation with c-myc. *EMBO J.* **8**, 749-755.

**Rumyantsev, P. P.** (1977). Interrelations of the proliferation and differentiation processes during cardiac myogenesis and regeneration. *Int. Rev. Cytol.* **51**, 187-273.

**Rumyantsev, P. P.** (1991). *Growth and Hyperplasia of Cardiac Muscle Cells*. London: Harwood Academic Publishers.

**Sassoon, D. A., Garner, I. and Buckingham, M.** (1988). Transcripts of α-cardiac and α-skeletal actins are early markers for myogenesis in the mouse embryo. *Development* **104,** 155-164.

**Sawai, S., Shimono, A., Hanaoka, K. and Kondoh, H.** (1991). Embryonic lethality resulting from disruption of both N-myc alleles in mouse zygotes. *New Biologist* **3**, 861-869.

**Sawai, S., Shimono, A., Wakamatsu, Y., Palmes, C., Hanaoka, K., and Kondoh, H.** (1993). Defects of embryonic organogenesis resulting from targeted disruption of the N-*myc* gene in the mouse. *Development* **117**, 1445-1455.

**Schwab, M., Alitalo, K., Klempnauer, K., Varmus, H. E., Bishop, J. M., Gilbert, F., Brodeur, G. M., Boldstein, M. and Trent, J.** (1983). Amplified DNA with limited homology to myc cellular oncogene is shared by human neuroblastoma cell lines and a neuroblastoma tumour. *Nature* **305,** 245-248.

**Spooner, B. S. and Wessells, N. K.** (1970). Mammalian lung development: interactions in primordium formation and bronchial morphogenesis. *J. Exp. Zool.* **175**, 445-454.

**Stanton, B. R., Reid, S. W. and Parada, L. F.** (1990). Germ line transmission of an inactive N-myc allele generated by homologous recombination in mouse embryonic stem cells. *Mol. Cell Biol.* **10**, 6755-6758.

**Stanton, B. R., Perkins, A. S., Tessarollo, L., Sassoon, D. A. and Parada, L. F.** (1992). Loss of N-myc function results in embryonic lethality and failure of the epithelial component of the embryo to develop. *Genes Dev.* **6**, 2235-2247.

**Tokuyasu, K. T.** (1990). Co-development of embryonic myocardium and myocardial circulation. In *Developmental Cardiology: Morphogenesis and Function* (ed. E. B. Clark and A. Takao), pp. 205-218. Mount Kisko, NY: Futura Publishing Co., Inc.

**Viragh, S. and Challice, C. E.** (1981). The origin of the epicardium and the embryonic myocardial circulation in the mouse. *Anat. Rec.* **201**, 157-168.

**Wenzel, A., Cziepluch, C., Hamann, U., Schuermann, J. and Schwab, M.** (1991). The N-myc oncoprotein is associated in vivo with the phosphoprotein Max(p20/22) in human neuroblastoma cells. *EMBO J.* **10**, 3703-3712.

**Wessells, N. K.** (1970). Mammalian lung development: interactions in the formation and morphogenesis of tracheal buds. *J. Exp. Zool.* **175**, 455-466.

**Wong, A. J., Ruppert, J. M., Eggleston, J., Hamilton, S. R., Baylin, S. B. and Vogelstein, B.** (1986). Gene amplification of c-myc and N-myc in small cell carcinoma of the lung. *Science* **233**, 461-464.

**Yamaguchi, T. P., Dumont, D. J., Conlon, R. A., Breitman, M. and Rossant, J.** (1993). Flk-1, a flt-1-related receptor tyrosine kinase is an early marker for heart and blood for endothelial cell precursors. *Development* in press,

**Zervos, A. S., Gyuris, J. and Brent, R.** (1993). Mxi1, a protein that specifically interacts with Max to bind Myc-Max recognition sites. *Cell* **72**, 223-232.

**Zimmerman, K., Yancopoulos, G. D., Collum, R. G., Smith, R. K., Kohl, N. E., Denis, K. A., Nau, M. M., Witte, O. N., Toran-Allerand, D., Gee, C. E., Minna, J. D. and Alt, F. W.** (1986). Differential expression of myc family genes during murine development. *Nature* **319**, 780-783.

(Accepted 30 June 1992)